Microscale Thermophysical Engineering, 6:3–13, 2002

1089-3954/02 $12.00 + .00

REPORTS

MOLECULAR DYNAMICS SIMULATION OF HETEROGENEOUS NUCLEATION OF A LIQUID DROPLET ON A SOLID SURFACE

Tatsuto Kimura and Shigeo Maruyama
Department of Mechanical Engineering, The University of Tokyo, Tokyo, Japan

Heterogeneous nucleation of a liquid droplet on a solid surface was simulated with the molecular dynamics method. Argon vapor was represented by 5,760 Lennard-Jones molecules and the solid surface was represented by one layer of 4,464 harmonic molecules with the constant temperature heat bath model using the phantom molecules. The potential parameter between a solid molecule and a vapor molecule was varied to reproduce several surface wettabilities. When the vapor-solid system was in equilibrium at 160 K, temperature of the solid surface was suddenly decreased to 100 K or 80 K by the phantom method. Observed nucleation rate, critical nucleus size and free energy needed for cluster formation were not much different from the prediction of the classical heterogeneous nucleation theory in case of smaller cooling rate. The discrepancy became considerable with the increase in cooling rate and with increase in surface wettability because of the spatial temperature distribution.

Liquid droplet nucleation on a solid surface is a very important phenomenon from the viewpoint of the dropwise condensation theory, and is also very interesting related to the nanotechnology such as quantum dot generation. We have simulated an equilibrium liquid droplet on a solid surface by the molecular dynamics method, and have clarified the relationship between the potential parameter of molecules and macroscopic quantities such as contact angle [1]. In addition, we have carried out a molecular dynamics simulation on the bubble nucleation process on a solid surface [2]. In the meantime, direct molecular dynamics simulations of the homogeneous nucleation process were performed by Yasuoka et al. for a Lennard-Jones fluid [3] and water [4], and a large discrepancy from classical nucleation theory was reported. Here, the heterogeneous nucleation of a liquid droplet on a solid surface was simulated directly by the molecular dynamics method and the nucleation rate was compared with the classical nucleation theory.

Received 13 September 2000; accepted 16 July 2001.
Address correspondence to Prof. Shigeo Maruyama, Department of Mechanical Engineering, The University of Tokyo, 7-3-1 Hongo, Bunkyo-ku, Tokyo 113-8656, Japan. E-mail: maruyama@photon.t.u.-tokyo.ac.jp

NOMENCLATURE

$c(n)$	number distribution function of clusters
f	function in classical heterogeneous nucleation theory
J	nucleation rate, cm^{-2} s^{-1}
k	spring constant, N/m
k_B	Boltzmann constant, J/K
m	mass, kg
n	cluster size
R_0	distance to nearest-neighbor molecules, m
r	radius or distance between two molecules, m
r_c	cutoff radius, m
S	supersaturation ratio
T	temperature, K
T_{wall}	set temperature of phantom molecules, K
α	damping factor, kg/s
γ_{lv}	surface tension of liquid–vapor interface, N/m
ΔG	free energy needed for cluster formation, J
Δt	time step, s
ξ	energy parameter of Lennard-Jones potential, J
ξ_{SURF}	depth of integrated effective surface potential, J
θ	contact angle, rad
ρ	number density, m^{-3}
σ	length parameter of Lennard-Jones potential, m
σ_F	standard deviation of exciting force, N
ϕ	potential function, J
ϕ_{SF}	shifted Lennard-Jones potential function, J

Subscripts and Superscripts

AR	argon
ave	average over nucleation period
e	saturated vapor
INT	interaction between argon and solid molecules
l	liquid
S	solid molecule
sim	simulation
th	classical nucleation theory
*	critical nucleus

SIMULATION METHOD

As shown in Figure 1, argon vapor consisting of 5,760 molecules in contact with a plane solid surface was prepared. The potential between argon molecules was represented by the well-known Lennard Jones (12–6) function as

$$\phi(r) = 4\xi\left[\left(\frac{\sigma}{r}\right)^{12} - \left(\frac{\sigma}{r}\right)^{6}\right] \tag{1}$$

where the length scale $\sigma_{AR} = 3.40 \times 10^{-10}$ m, the energy scale $\xi_{AR} = 1.67 \times 10^{-21}$ J, and the mass $m_{AR} = 6.63 \times 10^{-26}$ kg. We used the potential cutoff at $3.5\sigma_{AR}$ with the shift of the function for continuous decay [5].

$$\phi_{SF}(r) = 4\xi\left\{\left[\left(\frac{\sigma}{r}\right)^{12} - \left(\frac{\sigma}{r}\right)^{6}\right] + \left[6\left(\frac{\sigma}{r_c}\right)^{12} - 3\left(\frac{\sigma}{r_c}\right)^{6}\right]\left(\frac{r}{r_c}\right)^{2} - \left[7\left(\frac{\sigma}{r_c}\right)^{12} - 4\left(\frac{\sigma}{r_c}\right)^{6}\right]\right\} \tag{2}$$

The solid surface was represented by one layer of 4,464 harmonic molecules on an fcc (111) surface. Here, we set mass $m_S = 3.24 \times 10^{-25}$ kg, distance of nearest-neighbor molecules $R_0 = 2.77 \times 10^{-10}$ m, and spring constant $k = 46.8$ N/m from

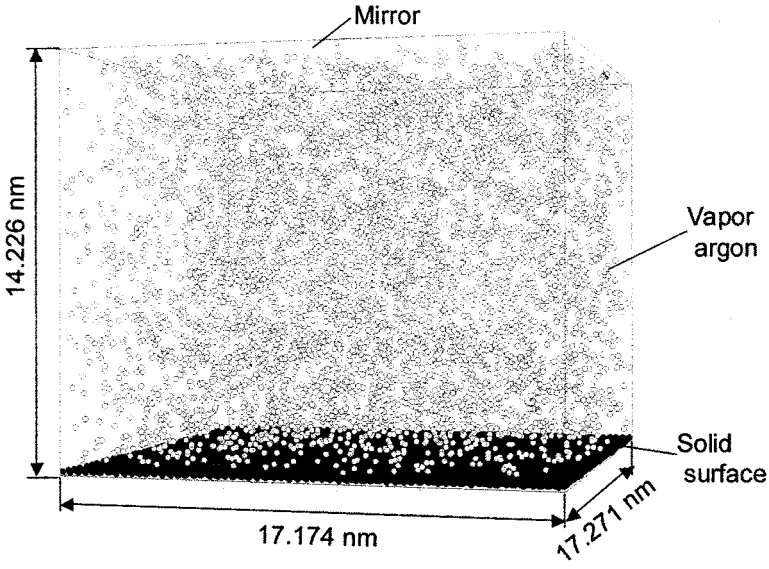

Figure 1. Simulation system.

the physical properties of solid platinum crystal. We have controlled the temperature of the solid surface by arranging a layer of phantom molecules beneath the "real" surface molecules. The phantom molecules modeled the infinitely wide bulk solid kept at a constant temperature T_{wall} with proper heat conduction characteristics [6, 7]. In practice, a solid molecule was connected with a phantom molecule with a spring of $2k$ in the vertical direction and springs of $0.5k$ in two horizontal directions. Then, a phantom molecule was connected to the fixed frame with a spring of $2k$ and a damper of $\alpha = 5.184 \times 10^{-12}$ kg/s in the vertical direction and springs of $3.5k$ and dampers of α in two horizontal directions. A phantom molecule was further excited by random force in a Gaussian distribution with the standard deviation

$$\sigma_F = \sqrt{\frac{2\alpha k_B T}{\Delta t}} \tag{3}$$

where k_B is Boltzmann's constant. This technique mimicked a constant-temperature heat bath which conducted heat from and to "real" surface molecules as if a bulk solid was connected.

The potential between argon and the solid molecule was also represented by the Lennard-Jones potential function. The length scale of the interaction potential σ_{INT} was kept constant at 3.085×10^{-10} m. In our previous study on a liquid droplet on the surface [1], we found that the depth of the integrated effective surface potential,

$$\xi_{\text{SURF}} = \frac{4\sqrt{3}\pi}{5} \frac{\xi_{\text{INT}} \sigma_{\text{INT}}^2}{R_0^2} \tag{4}$$

was related directly to the contact angle of the surface. Hence, we used various energy-scale parameters ξ_{INT} as in Table 1 to change the wettability.

Table 1. Calculation conditions

Label	ξ_{INT} [$\times 10^{-21}$ J]	θ [deg]	T_{wall} [K]	T_{ave} [K]	J_{sim} [cm^{-2} s^{-1}]	J_{th} [cm^{-2} s^{-1}]	J_{th} (local) [cm^{-2} s^{-1}]
E1	0.426	135.4	100	108	6.52×10^{20}	4.86×10^{21}	4.50×10^{21}
E2	0.612	105.8	100	114	3.45×10^{21}	4.47×10^{21}	1.45×10^{22}
E3	0.798	87.0	100	120	5.76×10^{21}	5.54×10^{20}	7.01×10^{22}
E1-L	0.426	135.4	80	111	3.96×10^{21}	2.23×10^{21}	7.62×10^{21}
E2-L	0.612	105.8	80	126	1.41×10^{22}	(10^{-134})	4.32×10^{22}
E3-L	0.798	87.0	80	129	2.96×10^{22}	N-A	1.44×10^{23}

The classical momentum equation was integrated by Verlet's leap-frog method with a time step of 5 fs. As an initial condition, an argon fcc crystal was placed at the center of the calculation domain. We used the velocity-scaling temperature control directly on the argon molecules for the initial 100 ps. Then, switching off the direct temperature control, the system was run for 500 ps with temperature control only from the phantom molecules until equilibrium argon vapor was achieved. After the equilibrium condition was obtained at 160 K, the set temperature of the phantom T_{wall} was suddenly lowered to 100 or 80 K, and the system was cooled from the solid surface. The supersaturation ratio

$$S = \frac{\rho}{\rho_e} \tag{5}$$

was evaluated to be about 6 and 40 at this stage, respectively.

RESULTS AND DISCUSSION

Variation of argon temperature and pressure in response to the wall temperature change for E2 in Table 1 are shown in the top panel of Figure 2. Here, we define a "cluster" as an interconnecting group of molecules whose intermolecular distances are less than $1.2\sigma_{AR}$. Change in number of monomers and maximum cluster size are plotted in Figure 2. In order to clarify the sensitivity to the threshold value of the cluster definition, the following analyses were repeated for another threshold value $1.5\sigma_{AR}$. As a result, no substantial differences were observed. After 500 ps from the start of the calculation, the solid surface was rapidly cooled by temperature control of phantom molecules, and the temperature of the argon gradually decreased afterward; then the formation and growth of clusters were recorded.

In Figure 3, snapshots of the nucleation process for E2 are shown. Here, for clarity, only clusters made of more than five molecules are shown. Initial small clusters appeared and disappeared randomly in space. Then larger clusters grew preferentially near the surface. Some of the largest clusters near the surface continued to grow until the end of the simulation. On the other hand, for the less wettable condition E1 in Figure 4, relatively large clusters grew without the help of surface, similar to homogeneous nucleation.

The cluster size distributions $c(n)$ for several instances (short-time average) are shown in Figure 5. Compared to the natural equilibrium distribution in Figure 5*a*, a

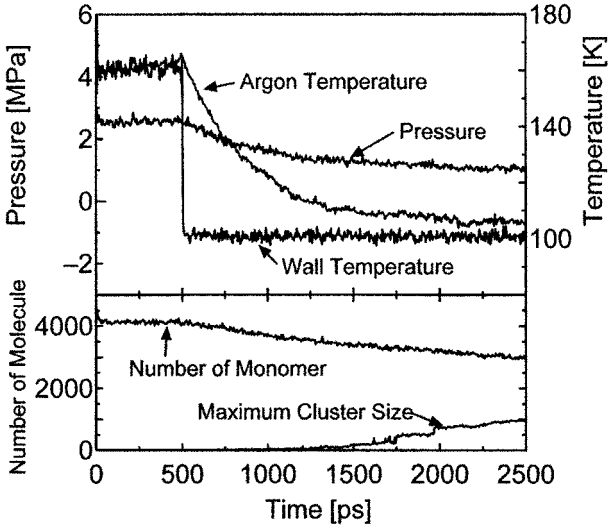

Figure 2. Variations of pressure, temperature, number of monomers, and maximum cluster size for E2.

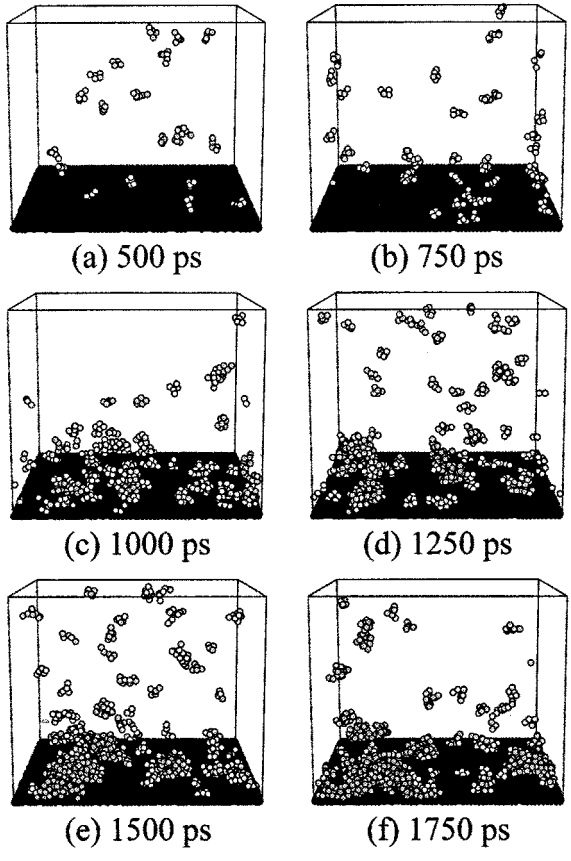

Figure 3. Snapshots of nucleation process for E2.

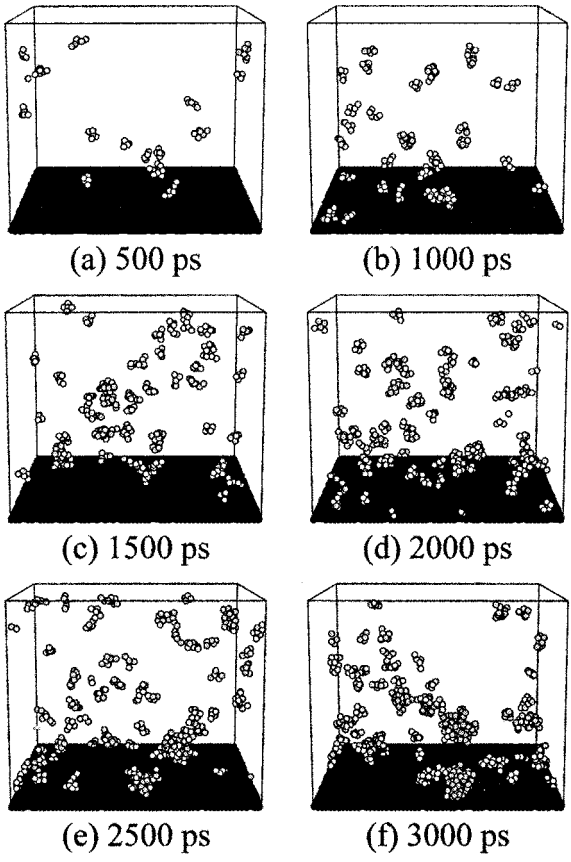

Figure 4. Snapshots of nucleation process for E1.

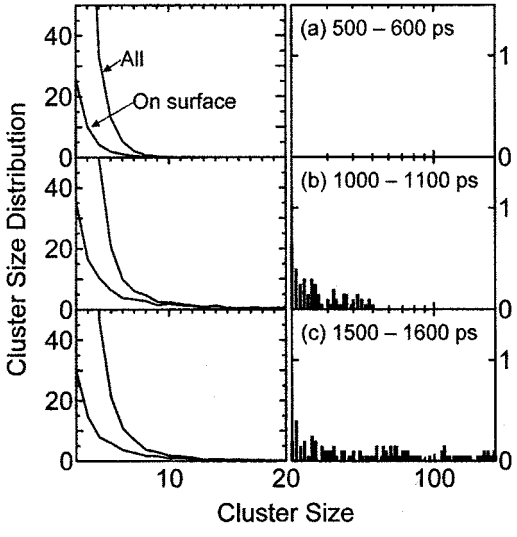

Figure 5. Clusters distribution for E2.

constant amount of increase of distribution for the size range beyond $n = 10$ can be conceived. The cluster size distribution in the range $1 < n < 20$ seemed to keep the same structure after 1,000 ps, and it was also observed that most clusters beyond $n > 10$ are principally on the surface for this wettability E2. The spikes in the larger cluster size range are due to the small number of clusters grown further from this quasi-equilibrium distribution in the range $1 < n < 20$.

The variations of the numbers of clusters larger than some thresholds are shown in Figure 6 as in the same manner as the results of homogeneous nucleation by Yasuoka et al. [3]. Dashed lines were fitted to the linear part of each increasing curve. These lines are almost parallel for the thresholds of over 20 or 30, and show that clusters that exceeded this size kept growing stably. It was proposed that the nucleation rate be estimated from the gradients of these lines [3]. Nucleation rate estimated from the average gradient of lines over 30, 40, and 50 becomes $J_{\text{sim}} = 3.45 \times 10^{21}$ cm^{-2} s^{-1}.

On the other hand, in the classical nucleation theory, nucleation rate J_{th} of the heterogeneous nucleation on a smooth solid surface is expressed as follows:

$$J_{\text{th}} = \rho^{2/3} \frac{\rho}{\rho_l} \frac{1 - \cos\theta}{2} \sqrt{\frac{2\gamma_{\text{lv}}}{\pi m f}} \exp\left(-\frac{\Delta G^*}{k_B T}\right)$$

$$f = \frac{1}{4}(2 - 3\cos\theta + \cos^3\theta) \tag{6}$$

$$\Delta G^* = \frac{16\pi r^3 f}{3(\rho_l k_B T \ln S)^2}$$

Using the average temperature T_{ave} and vapor density ρ in the period from 1,000 to 1,500 ps, in which the number of clusters changed linearly in Figure 6, the nucleation

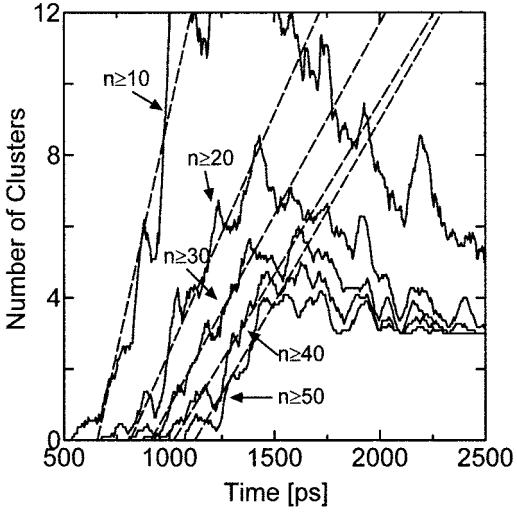

Figure 6. Variations of number of clusters larger than a threshold for E2.

rate was calculated to be $J_{\text{th}} = 4.47 \times 10^{21}$ cm^{-2} s^{-1}. Here, the values of the saturated vapor density ρ_e and liquid density ρ_l were calculated from the equation of state of a Lennard-Jones fluid [8], and the surface tension of the liquid–vapor interface γ_{lv} was employed from the physical properties of argon. Furthermore, the contact angle for each surface condition was estimated from our equilibrium simulation results [1]. The nucleation rate calculated from this simulation agreed with the classical nucleation theory very well, in clear contrast to the 7 orders of difference for the homogeneous nucleation by Yasuoka et al. [3]. The critical cluster size in the classical nucleation theory is given in the following equation:

$$n^* = \frac{32\pi\gamma^3 f}{3\rho_l^2 (k_B T \ln S)^3} \tag{7}$$

It was calculated to be 16.5 for current condition. In this simulation, it was estimated to about 20 from the change of the gradients of the lines in Figure 6, and the agreement was reasonable.

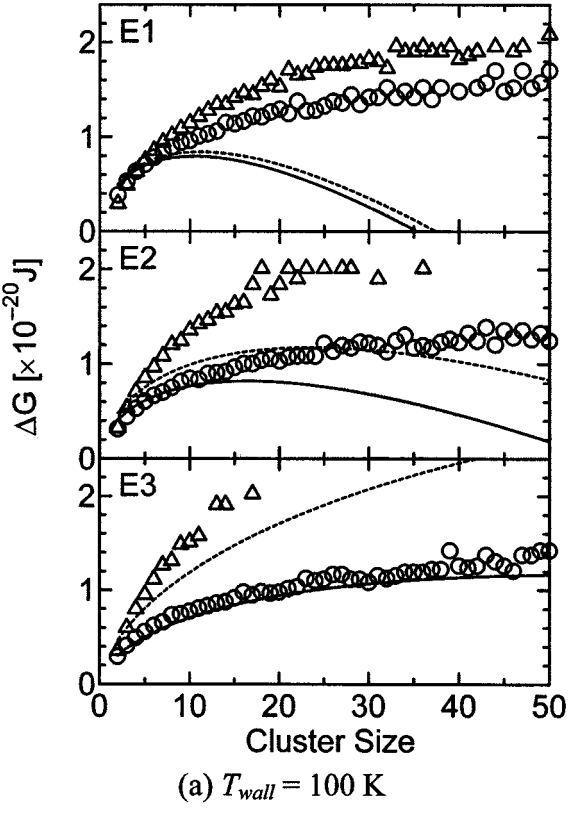

Figure 7. Cluster formation free energy.

Cluster size distribution in the range smaller than the critical nucleus n^* is given in following equation in the classical theory:

$$c(n) = \rho^{2/3} \exp\left(-\frac{\Delta G}{k_B T}\right) \tag{8}$$

The open circles in Figure 7 shows the free energy needed for cluster formation ΔG calculated using Eq. (8), from the average cluster distribution $c(n)$ such as in Figure 5 in the period in which clusters were forming stably. The solid line shows ΔG given in the heterogeneous nucleation theory as follows:

$$\Delta G = \left(4\pi r^2 \gamma - \frac{4}{3}\pi r^3 \rho_l k_B T \ln S\right) f \qquad n = \frac{4}{3}\pi r^3 \rho_l f \tag{9}$$

Triangles and broken lines show ΔG calculated from cluster distribution far from the solid surface and from the classical homogeneous nucleation theory, respectively. Considering that Eq. (8) is effective only in the size range smaller than the critical nucleus where

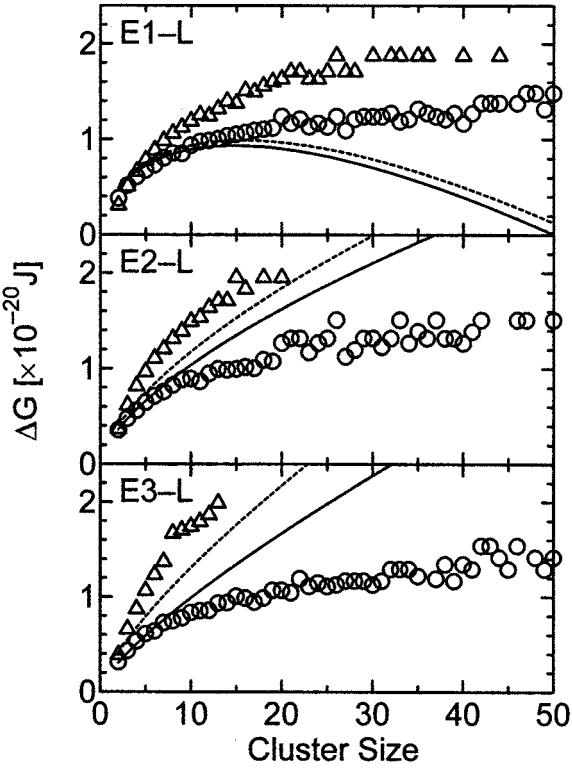

(b) T_{wall} = 80 K

Figure 7. (*Continued*)

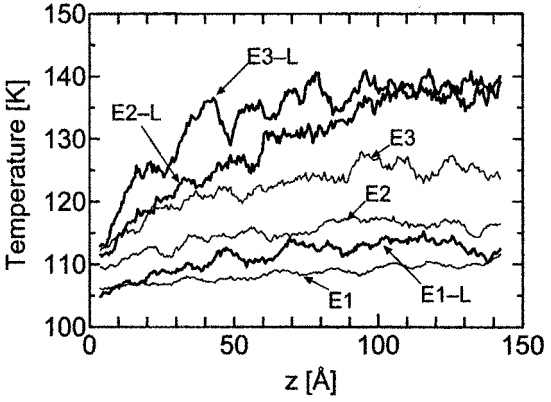

Figure 8. Temperature distribution during nucleation period.

ΔG is maximum in Eq. (9), it can be observed that ΔG from heterogeneous nucleation theory and from cluster distribution in contact with a solid surface almost agree for the simulations in which the set temperature of the solid surface T_{wall} was higher (100 K). Furthermore, ΔG from homogeneous nucleation theory and from cluster distribution far from the surface agreed well, though ΔG of simulation was slightly larger. The similar comparison of free energy by Yasuoka et al. [3] showed a remarkable difference in the simulation results from the classical theory.

On the other hand, for the simulations in which T_{wall} was lower (80 K), the difference between simulation and theory increased in E2-L and E3-L, though it almost agreed in E1-L, whose surface was less wettable. Actually, the theoretical value of the nucleation rate J_{th} for E2-L was extremely small, and the classical theory predicts no nucleation for the case of E3-L with a supersaturation ratio of 0.87. The problem was

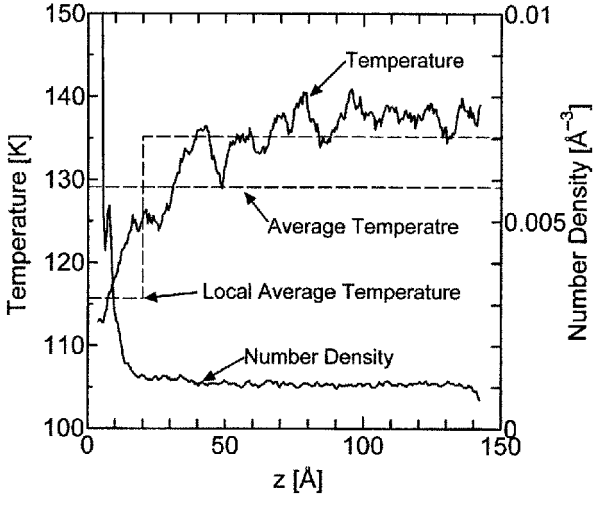

Figure 9. Density distribution and average temperature for E3-L.

in the steep vertical temperature distribution in our simulations. The vertical temperature distributions in the period in which clusters were stably forming were calculated as shown in Figure 8. Considerably large temperature gradient has been given in E2-L and E3-L, in which T_{wall} was lower and thermal boundary resistance [9] between the liquid and solid surface was smaller than in E1, E2, and E1-L. It can be understood that the difference from the classical nucleation theory tended to increase with the increase in the cooling rate because of the spatial temperature distribution.

Figure 9 shows density distribution and average temperature for E3-L. Since the clusters grew very near the surface in this case, the classical nucleation rate for the average temperature $0 < z < 20$ was calculated. The classical nucleation rate for this local average temperature agreed reasonably well with simulation results as shown in Table 1. The reason for the large discrepancy of homogeneous results by Yasuoka et al. [3] is not yet clear. It can be speculated that the cooling rate by collisions with buffer gas by Yasuoka et al. [3] may be too efficient.

CONCLUSION

We have successfully demonstrated the nucleation of a three-dimensional liquid droplet on a solid surface using the molecular dynamics method. The obtained nucleation rate, the critical nucleus size, and the free energy needed for cluster formation almost agreed with classical heterogeneous theory when the cooling rate was smaller or the solid surface was less wettable. Because of the spatial temperature distribution, the difference became larger with increase in cooling rate and surface wettability. However, with the definition of local average temperature, the simulation results were almost explained by the classical theory.

REFERENCES

1. S. Maruyama, T. Kurashige, S. Matsumoto, Y. Yamaguchi, and T. Kimura, Liquid Droplet in Contact with a Solid Surface, *Microscale Thermophys. Eng.*, vol. 2, no. 1, pp. 49–62, 1998.
2. S. Maruyama and T. Kimura, A Molecular Dynamics Simulation of a Bubble Nucleation on Solid Surface, *Int. J. Heat Technol.*, vol. 18, no. 1, pp. 69–74, 2000.
3. K. Yasuoka and M. Matsumoto, Molecular Dynamics of Homogeneous Nucleation in the Vapor Phase. I. Lennard-Jones Fluid, *J. Chem. Phys.*, vol. 109, no. 19, pp. 8451–8462, 1998.
4. K. Yasuoka and M. Matsumoto, Molecular Dynamics of Homogeneous Nucleation in the Vapor Phase. II. Water, *J. Chem. Phys.*, vol. 109, no. 19, pp. 8463–8470, 1998.
5. S. D. Stoddard and J. Ford, Numerical Experiments on the Stochastic Behavior of a Lennard-Jones Gas System, *Phys. Rev. A*, vol. 8, pp. 1504–1512, 1973.
6. J. C. Tully, Dynamics of Gas-Surface Interactions: 3D Generalized Langevin Model Applied to fcc and bcc Surfaces, *J. Chem. Phys.*, vol. 73, no. 4, pp. 1975–1985, 1980.
7. J. Blömer and A. E. Beylich, Molecular Dynamics Simulation of Energy Accommodation of Internal and Translational Degrees of Freedom at Gas-Surface Interfaces, *Surface Sci.*, vol. 423, pp. 127–133, 1999.
8. J. J. Nicolas, K. E. Gubbins, W. B. Streett, and D. J. Tildesley, Equation of State for the Lennard-Jones Fluid, *Mol. Phys.*, vol. 37, no. 5, pp. 1429–1454, 1979.
9. S. Maruyama and T. Kimura, A Study on Thermal Resistance over a Solid–Liquid Interface by the Molecular Dynamics Method, *Thermal Sci. Eng.*, vol. 7, no. 1, pp. 63–68, 1999.